IJE TRANSACTIONS B: Applications Vol. 36 No. 11, (November 2023) 2112-2123

International Journal of Engineering

Journal Homepage: www.ije.ir

A Numerical Study to Investigate Shear Behavior of High-strength Concrete Beams Externally Retrofitted with Carbon Fiber Reinforced Polymer Sheets

A. M. Jabbar*[a], D. H. Mohammed[b], Q. A. Hasan[b]

[a] *Civil Engineering Department, College of Engineering, Wasit University, Iraq*
[b] *Civil Engineering Department, University of Technology, Baghdad, Iraq*

PAPER INFO

Paper history:
Received 27 July 2017
Received in revised form 03 August 2023
Accepted 06 August 2023

Keywords:
Carbon Fiber Reinforced Polymer Sheets
Numerical Analysis
Abaqus
Beam Tolerance
High Strength Concrete

ABSTRACT

This paper aims to numerically investigate the structural behavior of reinforced high-strength concrete (HSC) beams retrofitted by Carbon Fiber Reinforced Polymer (CFRP) sheets after cracking. Six pre-cracked HSC beams retrofitted with CFRP sheets having identical reinforcement are numerically tested by four-point loading until failure using Abaqus software, besides two others without CFRP as control beams. CFRP sheets are attached on three beam sides in the shear span after cracking under 60 % of loading. Two shear span distances, two inclinations of CFRP sheets, and the number of sheets are adopted as parameters to compare with the experimental results obtained previously. Test results are matched with the practical findings to calibrate the Abaqus parameters. The results show that retrofitting the cracked beam by CFRP raised its tolerance to the applied load by a range of (13-36) % depending on the shear span to depth ratio and the arrangement of CFRP sheets. When the beam tends to fail in shear, the effect of CFRP is more pronounced than when it tends to fracture in flexure. The inclined sheets are more effective than the vertical ones. Furthermore, two additional parameters are regarded to clarify their effects on the behavior of retrofitted beams: sheet width and concrete compressive strength. Altering the CFRP width does not affect the tolerance, whereas increasing concrete compressive strength raises the beam loading.

***doi**: 10.5829/ije.2023.36.11b.15*

1. INTRODUCTION

Several causes contribute to the necessity of retrofitting the existing facilities, such as strength loss due to corrosion, erosion, or deterioration caused by nature effects. Changing the use, expanding the facility, and upgrading the structure to resist higher loads also require correcting design or construction weaknesses [1, 2]. Retrofitting of facilities is a common practice; therefore, retrofitting approaches have been offered and evolved over years of practical and experimental work. The finding of the method used to retrofit a structural component relies on financial regard and the practicality of the assumed approach. However, choosing an inappropriate retrofitting manner can worsen the structure's function or even lastly causes failure [3].

Modern installations, like buildings, towers, and bridges, may deteriorate for different reasons. These installations are pricey to rebuild, and the construction time may cause trouble for many users. Therefore, it is significant to maintain enduring structures with long lifetimes and low maintenance costs. The most common manner for enhancing lifetime and durability is upgrading [4]. Establishments can be boosted to meet the changing demands or restored to an initial implementation status. The implementation status indicates load-carrying capacity, durability, operation, and aesthetic impression [5]. Retrofitting is usually complicated way because the structural components are already established. Therefore, it is not easy to reach the areas that require retrofitting [6]. Conventional approaches, including shotcrete, steel overlays, and post-

*Corresponding Author Email: adilmahdi@uowasit.edu.iq
(A. M. Jabbar)

Please cite this article as: A. M. Jabbar, D. H. Mohammed, Q. A. Hasan, A Numerical Study to Investigate Shear Behavior of High-strength Concrete Beams Externally Retrofitted with Carbon Fiber Reinforced Polymer Sheets, ***International Journal of Engineering, Transactions B: Applications,*** Vol. 36, No. 11, (2023), 2112-2123

tensioned cables, usually need broad space [7, 8]. Consequently, materials having higher strength and better application procedures than conventional ones should be most suitable for retrofitting and of high benefits in practice [9].

Recently, the most appropriate material used to retrofit and strengthen installations is Fiber Reinforced Polymer Composite (FRP) [10]. That material is a desirable rehabilitation substance due to its characteristics, like high strength-to-weight ratio and noncorrosive features that permit enhancing installation life [11]. Carbon FRP (CFRP) is a good strengthening fabric due to its distinguished tensile strength and stiffness compared to other composite substances [12, 13]. Externally bonded CFRP can use to repair and strengthen damaged structural elements. In such structures, the complete strengthening work takes a little while, which is faster than an alternative of replacing the beams with new ones [14]. The polymer matrix is applied to tie the fibers together, transfer the forces among the fibers and protect them from external effects. The shear strength erected between the fibers depends on the tie-matrix properties [4, 11, 15]. Therefore, it is significant that the matrix must have the ability to maintain higher strains than the fibers. If not, there will be cracks in the matrix before the fibers fail, and the fibers will be unprotected [14, 16].

This paper describes the potential and weakness of adding composite materials to retrofit cracked concrete beams. The prime aims are to investigate the impact of using CFRP sheets to rehabilitate cracked high-strength concrete beams on its shear behavior. The parameters include shear span-to-depth ratio (a/d), CFRP sheet number, and orientation.

2. EXPERIMENTAL DATA FOR SIMULATION OF RETROFITTED BEAMS

Practically performed RC beams were chosen to capture the required data to simulate the retrofitted beams for comparitive study. Eight simple supported beams cast with high-strength concrete were performed by Al-Saeedi [17]. The beams were tested under a four-point load. All beams have an equal cross-section of (150x220) mm and a length of 1500 mm. The beams are designed according to ACI-318-19 [18] to avoid flexural failure using a 3-rebar of 20 mm diameter at the bottom and a 3-rebar of 12 mm diameter at the top so that shear is controlled, as shown in Figure 1. A concrete cover of 20 mm is applied for all sides of the beam cross-section. The tests were performed after curing in water for 28 days according to ASTM C31/C31 M-19 [19]. Three parameters were adopted in the experimental work. These are the shear span to depth ratio (a/d), CFRP sheet angle, and the number of CFRP sheets.

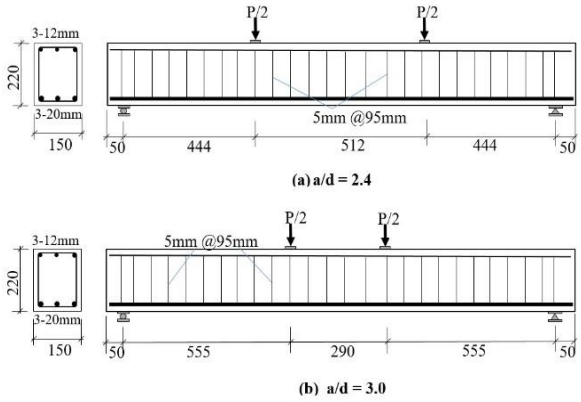

Figure 1. Details of beams' dimensions and reinforcement

The beams were categorized into two groups according to the a/d ratio. The first group had a/d = 2.4 while the second had a/d of 3.0. Each group consisted of four beams, the first beam (BA) without CFRP sheets is cast as a control beam, and the second (BRA1) had two CFRP sheets as a U-Shape on the beam sides and bottom at the mid-distance between the support and the nearby loading point with 90° configurations. A third beam (BRA2) had two CFRP sheets as U-Shape at the same place as the beam (BRA1) but with a 45° configuration. The fourth one (BRA3) had three CFRP sheets as U-Shape on the beam sides at the mid-distance between the support and the loading point with 45° configurations. The CFRP sheets had a 40 mm width and 0.131 mm thickness. Each group was represented with an a/d ratio [17]. Figure 2 illustrates the configuration of CFRP sheets on the beams.

2. 1. Materials and Mix Proportions Ordinary Portland cement (ASTM type I), natural fine aggregate with a 2.61 specific gravity, and natural crushed gravel with a maximum size of 10 mm and specific gravity of 2.58 were used for the mix. Silica fume of 91 % silicon dioxide with a surface area of 20000 m^2/kg is added as a cementitious material. Glenium 54, as a high-range water reducer (HRWR), is used as a percentage of cement weight to modify the workability of the mixture at a slump of 100 mm. The w/c ratio is constant at 0.28 [17]. Mix proportions and mechanical properties of concrete are listed in Table 1.

SikaWarp-300 C/60 woven carbon fiber fabric for concrete strengthening is used for retrofitting the beams experimentally. The CFRP does not exhibit plastic behavior before rupture, where the tensile stress-strain relationship is linear until failure. Therefore, CFRP failure is sudden and catastrophic. The tensile strength of carbon fiber is 3900 MPa, the elastic modulus is 230 GPa, and the elongation percentage at rupture is 1.5 %. Sikadur-330 epoxy glue is used as a bonding material for CFRP sheets. It has 30 MPa tensile strength and 4500

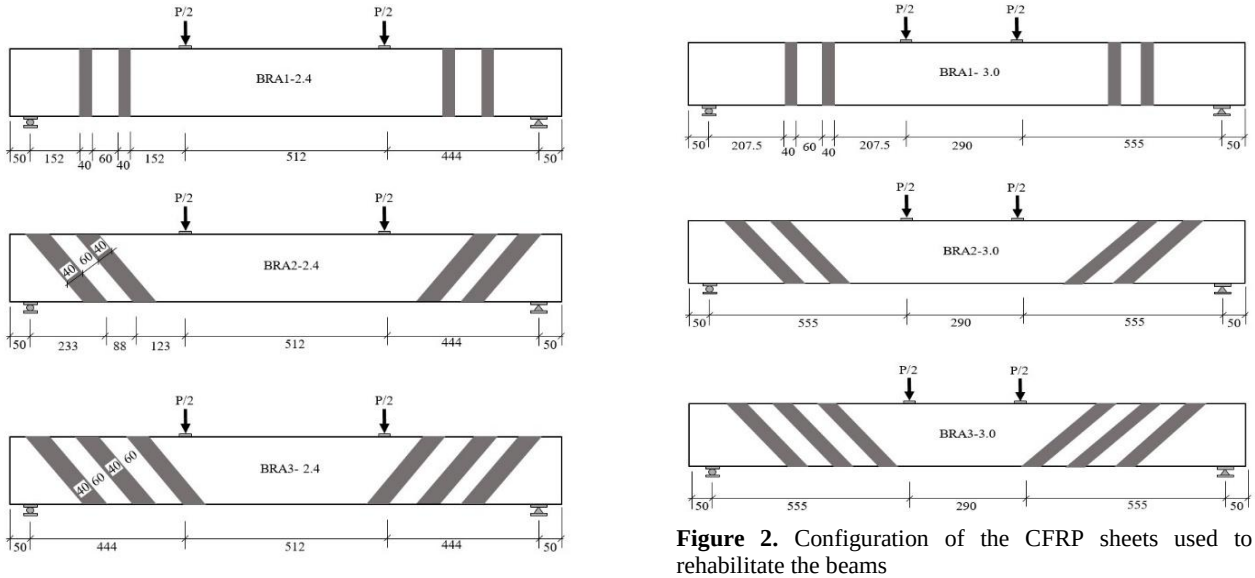

Figure 2. Configuration of the CFRP sheets used to rehabilitate the beams

TABLE 1. Mix proportioning and concrete strength

Mix Proportion						
Material	**Cement (kg/m^3)**	**Silica fume (kg/m^3)**	**Sand (kg/m^3)**	**Crushed gravel (kg/m^3)**	**w/cm**	**HRWR (% of cement)**
Quantity	450	50	750	1000	0.28	2.8
Concrete Mechanical Properties						
f'c 7-day		**f'c 28-day**		**fspt., MPa**		**Ec, MPa**
65		72.5		6.0		41770

MPa elastic modulus in tension. Three rebar diameters are used for reinforcing the beams, as shown in Figure 1. Table 2 lists the mechanical properties of steel rebars.

All beams were tested before retrofitting under four-point loading in the first test stage without any strengthening or retrofitting with CFRP to reach the specified damage. The beams arrived at the degree of the damaged ratio at 60% of the ultimate load of the control beam. Then, the beams were retrofitted using CFRP sheets [17].

3. EXPERIMENTAL RESULTS

Concrete cylinders of (150 x 300) mm were cast from the same concrete batch used for casting the beams as control specimens and tested at the same age as the beam test. Three cylinders were cast with each beam and the average value was considered. The average compressive strength was 72.5 MPa and the splitting tensile strength was 6.0 MPa, as illustrated in Table 1.

TABLE 2. Mechanical properties of steel rebars

Nominal rebar diameter, mm	Yield stress, MPa	Tensile strength, MPa	Elongation
20	450	667	0.00229
12	520	611	0.00263
5	480	590	0.00243

At initial loading, all beams elastically behaved up to about 20 % of ultimate load when first cracking appeared with proportional deflection. The first crack occurred in the tension zone at the lower portion between loading points. Then, flexural cracks vertically propagated to a short distance due to increasing tensile stresses. However, the elastic behavior continued, even after the initiation of flexural cracks, up to a load of approximately 40% of the ultimate loading. The stresses resulting from the imposed load on the beam were transmitted initially to the tensile region. When the steel rebars contributed to bearing stresses, they were redistributed to the shear zone. Shear cracks propagated diagonally between supports and the adjacent loading point. The first diagonal crack was observed at the loading level (40-52) % of the ultimate load, as shown in Figure 3. Upon increasing the loading, shear cracks expanded and extended down towards the support and up to the point load.

All beams were preloaded to 60 % of the ultimate load, except the control one, in which the loading continued to fail. The others were rehabilitated using the CFRP sheets. The test results are listed in Table 3.

4. NUMERICAL ANALYSIS OF THE BEAMS

Despite the symmetry, the beams are simulated with their entire dimensions. Abaqus CAE is used for the Finite Element Analysis (FEA) of beams. The analysis was performed in two static general steps by displacement control method.

4. 1. Numerical Simulation of Beams The beam components simulated in Abaqus consist of concrete, steel rebars, CFRP sheets, and steel plates for supporting and loading the beam. The concrete beam and steel plates are discretized into C3D8R as homogenous solid elements. C3D8R is a 3-dimensional continuum element that has 8 nodes as a brick element where each node has 3 degrees of freedom in the three directions with reduced integration upon iteration process to calculate the stiffness matrix for each load increment [20, 21].

The rebars are discretized by the T3D2 truss element that has 2 nodes with 3 degrees of freedom per node. The CFRP sheets are discretized as a composite layup shell of the S4R element, which is a 4-node doubly curved thin shell with reduced integration [22].

The steel plates are considered rigid bodies to transfer the loading to the beam without distortion. The steel rebars are assigned as embedded regions inside the host region of the concrete beam. The CFRP sheets are constrained as a tie between two surfaces, the master surface is the concrete beam, and the slave one is the sheet [22-24]. The interaction between steel plates and the concrete beam is a surface-to-surface contact type with two properties; tangential behavior with a friction coefficient of 0.45 and normal behavior of hard contact with no penetration between the adjacent surfaces. The boundary conditions are created at the initial step. The lower supporting plate is designated as fixed boundary conditions, which are assumed for the supporting plates by preventing the translations and rotations in all directions.

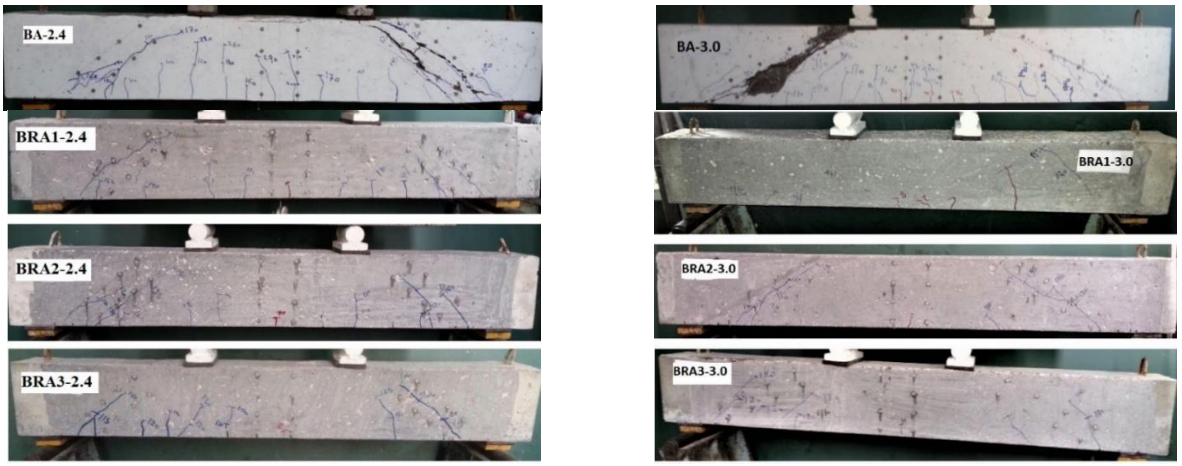

Figure 3. Cracking of the experimental beams at the first stage of loading before retrofitting [17]

TABLE 3. Test results of the beams [17]

Beam ID	CFRP sheet	a/d	Cracking State		Peak State		Failure Mode
			Pcr	Δcr	Pu	Δu	
BA-2.4	--	2.4	55	0.92	260	13.35	Diagonal shear
BRA1-2.4	2 at 90	2.4	53	0.71	310	14.25	Diagonal shear and debonding CFRP
BRA2-2.4	2 at 45	2.4	50	0.75	335	13.05	Debonding CFRP sheets
BRA3-2.4	3 at 45	2.4	58	0.63	375	13.58	Compression failure + debonding CFRP
BB-3.0	--	3.0	38	0.90	225	12.15	Diagonal shear
BRB1-3.0	2 at 90	3.0	42	0.85	260	12.53	Diagonal shear and debonding CFRP
BRB2-3.0	2 at 45	3.0	47	0.94	275	12.90	Debonding CFRP sheets
BRB3-3.0	3 at 45	3.0	48	0.95	317	13.20	Compression failure + debonding CFRP

A download vertical displacement is applied on upper steel plates to simulate the loading in a displacement control method in two loading steps. The first loading was up to 60 % of the ultimate load of the control beam. The other loading step was to complete the loading on the beam. All beam components are seeded into 20 mm mesh size, as shown in Figure 4.

4. 2. Concrete, Steel Rebar, and CFRP Sheet Modelling The compressive strength used to simulate the concrete in the beam is 72.5 MPa, and the cracking stress is assumed to be 40 % of compressive strength as the experimentally obtained value. Therefore, the concrete is numerically simulated by two behaviors as is required in Abaqus; linear behavior by the elastic modulus and Poisson's ratio. The plastic behavior is described in two stages; strain hardening to the concrete strength and strain softening after peak strength. The Concrete Damage Plasticity (CDP) model is adopted to define the plastic behavior of concrete after cracking [25, 26]. The compressive stress-strain relationship of the concrete is formulated using Hognestad equation as described in Equation (1) below, which awards a reasonable approach to the experimental results;

$$\sigma_c = 2f'_c\left[\frac{\varepsilon_c}{\varepsilon_{co}} - \left(\frac{\varepsilon_c}{\varepsilon_{co}}\right)^2\right] \quad (1)$$

where: σ_c is the concrete compressive stress at the corresponding strain ($\mathcal{E}_c$) in MPa, ε_c is the concrete strain at compression, and ε_{co} is the strain at compressive strength. The modulus of elasticity and inelastic strain are formulated using Euro code2-2004 [27] approach as illustrated in the following equations:

$$E_c = 3320\sqrt{f'_c} + 6900 \quad (2)$$

$$\varepsilon_{pl.} = \varepsilon_c - \frac{\sigma_c}{E_c} \quad (3)$$

E_c is the elastic modulus of concrete in MPa. $\varepsilon_{pl.}$ is the plastic strain. The damage parameter (dc) in compression is defined as follows;

$$d_c = 1 - \frac{\sigma_c}{f'_c} \quad (4)$$

The five parameters required to define the failure surface of the elements, including eccentricity, biaxial to uniaxial stress, and the shape of failure, were set as default values regarded in Abaqus. However, the dilation angle and viscosity were calibrated to obtain the maximum loading of the beams recorded in the experimental works, as illustrated in Table 4 [28]. These five parameters present concrete cracking in Abaqus. The rebar stress-strain relationship was represented by elastic-perfect plastic behavior. Table 4 illustrates the mechanical properties and parameters of concrete and steel rebars used to simulate the beams in Abaqus [29].

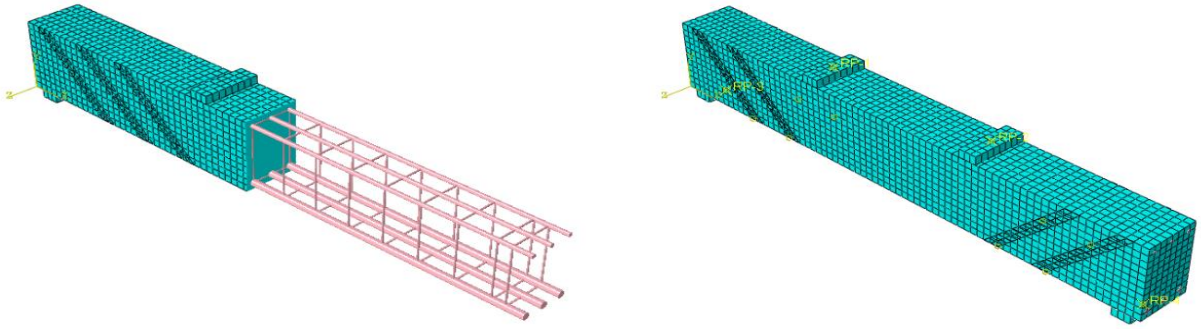

Figure 4. Simulation of concrete beams via Abaqus software

TABLE 4. The properties of materials used to simulate the retrofitted beams

Material	Properties								
concrete	Elastic modulus, Ec			35168.78 MPa		Poisson ratio		0.18	
	Compressive strength			72.5 MPa		Tensile strength		6.9 MPa	
	Dilation angle, ψ		Eccentricity, Ɛ	biaxial to uniaxial stress ratio, fbo/fco		Shape Parameter, K		viscosity parameter, μ	
	45		0.1	1.16		0.677		0.02	
Steel rebars	Diameter = 20 mm			Diameter = 12 mm			Diameter = 5 mm		
	Es	Yield stress	Poisson's ratio	Es	Yield stress	Poisson's ratio	Es	Yield stress	Poisson's ratio
	200 GPa	450 MPa	0.3	200 GPa	520 MPa	0.3	200 GPa	480 MPa	0.3

The CFRP sheets are simulated in elastic and plastic status. Lamina type is used for elastic behavior, and Hashin Damage is used for plastic behavior to define the damage features of fiber-reinforced composites [30]. The calibrated data depends on the experimental values provided by the manufacturer. The mechanical properties of the CFRP sheets are listed in Table 5.

Where E1 and E2 are the elastic modulus in the x and y-directions, μ12 is the Poison's ratio in the xy-plane, G12, G13, and G23 are the shear modulus in xy, xz, and yz-directions [25, 31].

4. 3. FEA Results of the Beams The analysis results of all beams are illustrated in Table 6. The cracking load was approximately equal for all beams in each group. At a/d of 2.4, the cracking load was about 58 kN, while at a/d of 3.0, it was about 45 kN. At the cracking state, the experimental results recorded a lower load than the finite element results by a range of (85-99) % for a/d = 2.4. For a/d = 3.0, the variation between experimental and FE loads ranges between (85-106) %, as shown in Table 6. These variations may be due to several reasons, such as the micro-cracks normally occurring in concrete due to shrinkage, handling the beams for testing, and environmental effects. However, concrete simulation in FE does not contain such micro cracks. Other reasons relate to the materials' definition in the Abaqus, which depends on the stress-strain relationship at the cracking state.

At the ultimate state and for a/d = 2.4, the variation in load occurred due to the impact of CFRP sheets and their orientations. The increment in ultimate load was 17 %, 23 %, and 36 % upon using 2 CFRP sheets at 90, 2 CFRP sheets at 45, and 3 CFRP sheets at 45, respectively, over the control beam maximum load. For a/d = 3.0, the increment in the ultimate load was 13 %, 19 %, and 35 % upon using 2 sheets of CFRP at 90, 2 CFRP sheets at 45, and 3 CFRP sheets at 45, respectively, over the control beam maximum load, as illustrated in Figure 5. Based on the findings of this study, it appears that utilizing 3-CFRP sheets in rehabilitation efforts yields the highest increase in loading capacity. This information could be valuable

TABLE 5. Mechanical properties of the CFRP sheets used in Abaqus

Elastic	**E1, MPa**	**E2, MPa**	**μ12**	**G12, MPa**	**G13, MPa**	**G23, MPa**
	131900	9510	0.326	5270	7030	3390
Plastic	**Type**			Hashin Damage		
	Long. tensile strength	Long. compressive strength	Transverse tensile strength	Transverse compressive strength	Long. shear strength	Transverse shear strength
	1328 MPa	1064 MPa	70.9 MPa	221 MPa	71.2 MPa	94.5 MPa
	Damage Evolution		**Type**	Energy	**Softening**	Linear
	Longitudinal tensile fracture energy		Longitudinal compressive fracture energy	Transverse tensile fracture energy	Transverse compressive fracture energy	
	0.33 mJ/mm^2		0.33 mJ/mm^2	2.00 mJ/mm^2	2.00 mJ/mm^2	

TABLE 6. Results of FEA for the beams

Beam ID	**CFRP sheet**	**a/d**	**Cracking State**						**Peak State**					
			Exp.		**FEA**		**Pcr (Exp/ FEA)**	**Δcr (Exp/ FEA)**	**Exp.**		**FEA**		**Pu (Exp/ FEA)**	**Δu (Exp/ FEA)**
			Pcr, kN	**Δcr, mm**	**Pcr, kN**	**Δcr, mm**			**Pu, kN**	**Δu, mm**	**Pu, kN**	**Δu, mm**		
BA-2.4	-	2.4	55	0.92	57.7	0.74	0.95	1.24	260	13.35	272.8	13.25	0.95	1.01
BRA1-2.4	2 at 90	2.4	53	0.71	58.4	0.74	0.91	0.96	310	14.25	319.6	15.78	0.97	0.90
BRA2-2.4	2 at 45	2.4	50	0.75	58.5	0.74	0.85	1.01	335	13.05	334.9	16.41	1.00	0.80
BRA3-2.4	3 at 45	2.4	58	0.63	58.8	0.74	0.99	0.85	375	13.58	370.7	17.81	1.01	0.76
BB-3.0	-	3.0	38	0.90	44.8	0.66	0.85	1.36	225	12.15	223.4	11.54	1.01	1.05
BRB1-3.0	2 at 90	3.0	42	0.85	44.9	0.66	0.94	1.29	260	12.53	252.1	14.01	1.03	0.89
BRB2-3.0	2 at 45	3.0	47	0.94	44.9	0.67	1.05	1.40	275	12.90	265.8	14.82	1.03	0.87
BRB3-3.0	3 at 45	3.0	48	0.95	45.2	0.66	1.06	1.44	317	13.20	301.1	18.23	1.05	0.72

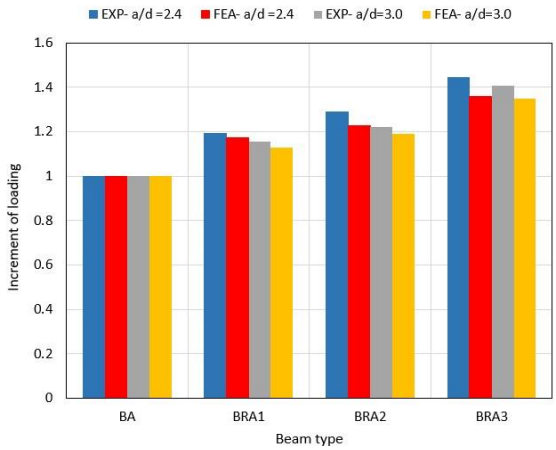

Figure 5. Increment in loading due to adding CFRP sheets

for those looking to improve the strength and durability of structures or materials. For a/d = 2.4, the beam tends to fail in shear. Therefore, the action of CFRP sheets in enhancing the shear capacity of the beam was more pronounced than that of a/d = 3.0. When the stresses are redistributed to the shear span on both sides of the beam, and this case occurs faster when a/d is 2.4, the effect of the CFRP sheets appears more clearly in enhancing the shear resistance. In the case of a/d is 3.0, the stresses transmitted to the shear span are less. That means the stress redistribution is between the tension area below the mid-span of the beam and the shear span. Then the effect of CFRP sheets is less because they resist the shear and do not resist the tensile due to their absence in the tension zone. Therefore, the beam tends to fail in flexure in the case of a/d is 3.0.

Generally, the use of inclined CFRP sheets is more effective than perpendicular ones in terms of loading and specifically for shear in beams. That could be interrupted as the CFRP sheets are perpendicular to the path of the inclined cracks of shear, which hinder the progression of cracks.

4. 4. Beams' Deflection Results The cracking deflection of FEA was equal for all beams in the case of a/d=2.4 and 3.0, as shown in Table 6. On the other hand, the ratio of experiment to FEA deflection at the cracking state ranges between (0.84-1.24) for a/d = 2.4, while for a/d = 3.0, the experimental cracking deflection was higher than the FE one. That may be due to the constraint provided by FE simulation.

At the ultimate state, the ratio between the experimental to FEA deflection ranges between (0.81-1.05). Generally, the increment in deflection recorded in the case of a/d=3.0 is higher than that of a/d = 2.4. The action of CFRP sheets on deflection occurred after the cracking state. For a/d=2.4, the three inclined CFRP sheets increased deflection by 27 % over that of the control beam, while for a/d =3.0, the three inclined CFRP sheets raised the deflection by 41 %. The increment in deflection upon using 2/90 and 2/ 45 CFRP sheets was 19% and 24% at a/d = 2.0, and 21%, 28%, at a/d =3.0, as shown in Figure 6.

The increment in deflection for a/d=3.0 is more than that for a/d=2.4. That is because the beam with a/d=3.0 tends to fail in flexural, while the one with a/d = 2.4 tends to fail on shear. The distribution of stresses in the first case is partially focused on a flexural zone, while the stresses are redistributed to the shear span in the second case.

Figures 7 and 8 show the load-deflection relationship of the beams. The behavior of beams was similar in both groups up to about 100 kN load, which is greater than the cracking load of 58 kN for a/d=2.4 and 45 kN for a/d = 3.0. This behavior is consistent with what was recorded in the experimental behavior of the beams. Then the behavior altered according to the number and configuration of CFRP sheets. Since all rehabilitated beams were manufactured with the same concrete and

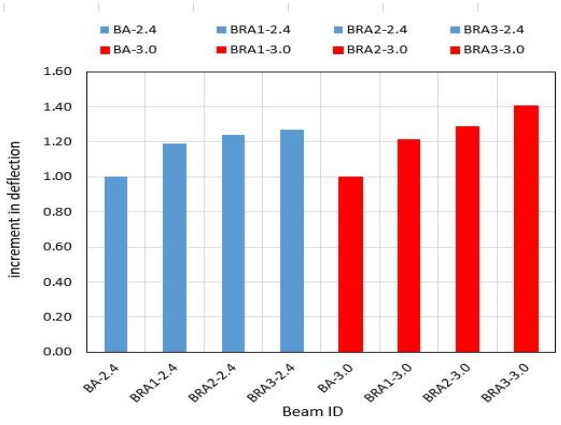

Figure 6. The percentage of deflection variation for all beams

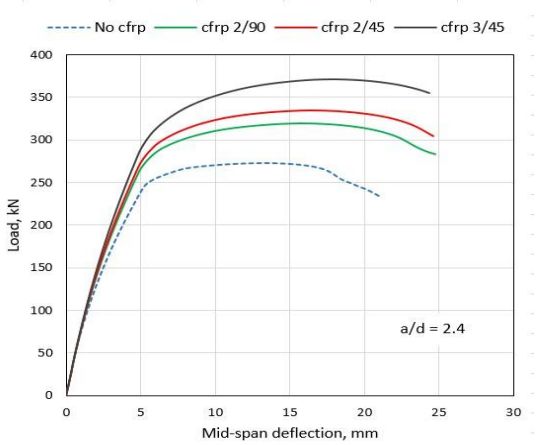

Figure 7. Load-deflection of beams with a/d=2.4

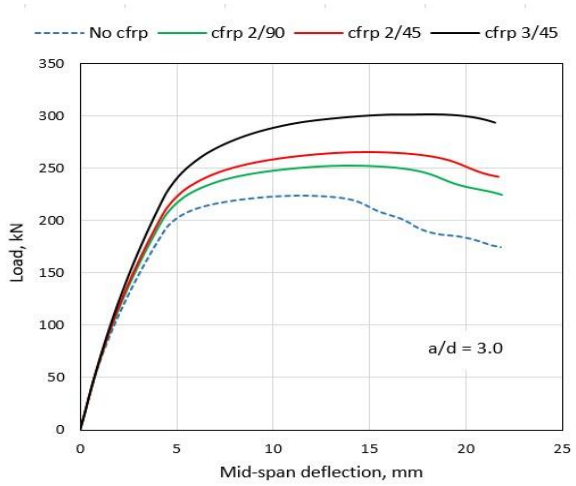

Figure 8. Load-deflection of beams with a/d=3.0

similar reinforcement, the variation in the behavior and ultimate loads depends on the CFRP sheets.

On the other hand, all beams did not exhibit high ductility after peak load. That could be because the behavior of CFRP is linear to failure.

4. 5. Impact of a/d Ratio on Beam Behavior When a/d decreases, the tolerance of the beam to the applied loads improves. The load capacity of the control beam increases by 22 % upon reducing a/d from 3.0 to 2.4. In the case of retrofitted beams by CFRP, the beam tolerance increases by (23-27) % at a/d =2.4. This behavior is because the beam bears more shear loads, and the presence of CFRP helps it increases endurance**.**

4. 6. Steel Rebar Stresses In all beams with a/d=2.4 and 3.0, the longitudinal rebars in the tension and compression zone have yielded at the peak load, as illustrated in Figure 9. That means the beam failed due to the yielding of the tensile rebars before the fracturing of concrete in compression zone because the CFRP sheets enhanced the shear resistance of the beam and that increases the stress in the flexural region.

On the other hand, the vertical stirrups do not yield along the shear spans between the supports and adjacent loading points. However, in beams with 2 CFRP at 45, 2 CFRP at 90, and 3 CFRP at 45 with a/d=3.0, the mid-span stirrup yield at the upper portion near the compression zone. That is due to the fracturing of the concrete at the compression region after reaching the ultimate concrete strain, as shown in Figure 10.

4. 7. Crack Pattern For all beams that were retrofitted by CFRP sheets with a/d = 2.4 and 3.0, the failure was due to diagonal shear cracking and debonding the CFRP sheets except for the one with 3 CFRP sheets at 45 and a/d=3.0, where they failed due to concrete

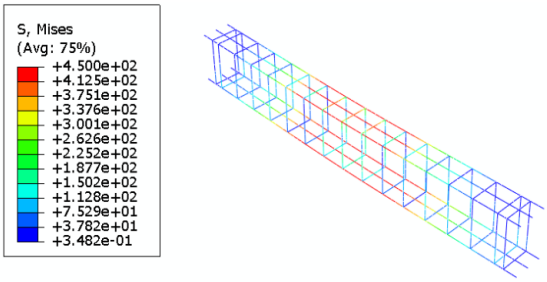

Figure 9. Stress distribution in steel rebars at the ultimate load

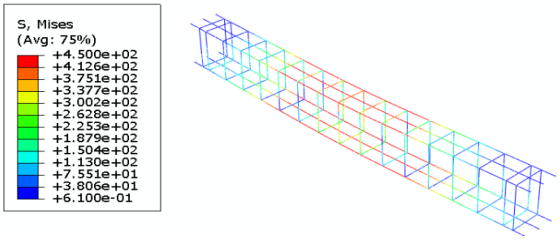

Figure 10. Yielding of the middle stirrup in beams BRA1-3.0, BRA2-3.0, and BRA3-3.0

compression fracture, as shown in Figure 11. That indicates that the number of inclined CFRP affects changing the behavior of the beam and its failure pattern. That behavior is consistent with experimental failures as mentioned in Table 3.

Generally, the CFRP sheets attached to the shear spans of the beam enhance the beam load capacity in shear and may alter the failure from diagonal shear to concrete compression fracture. Figure 11 illustrates the cracking pattern that occurs in the analyzed beams compared to the experimental cracking of the counterpart beams, in which the agreement of the type of failure is observed in the experimental beams and the ones simulated by Abaqus.

5. PARAMETRIC STUDY

5. 1. Effect of Variation of CFRP Sheet Width The first parameter considered was changing the CFRP sheet width. Two additional widths were examined to show their effect on beam behavior. The width changed to 80 mm and 120 mm, and they were placed in the same positions on the sides and bottom of the beam as in the case of 40 mm wide CFRP. However, changing the CFRP width did not affect the beam maximum loading and the corresponding deflection, as shown in Figure 12.

5. 2. Effect of Altering Concrete Compressive Strength Undoubtedly, changing the concrete strength affects the beam behavior; but how is the effect in the case of retrofitted beams?

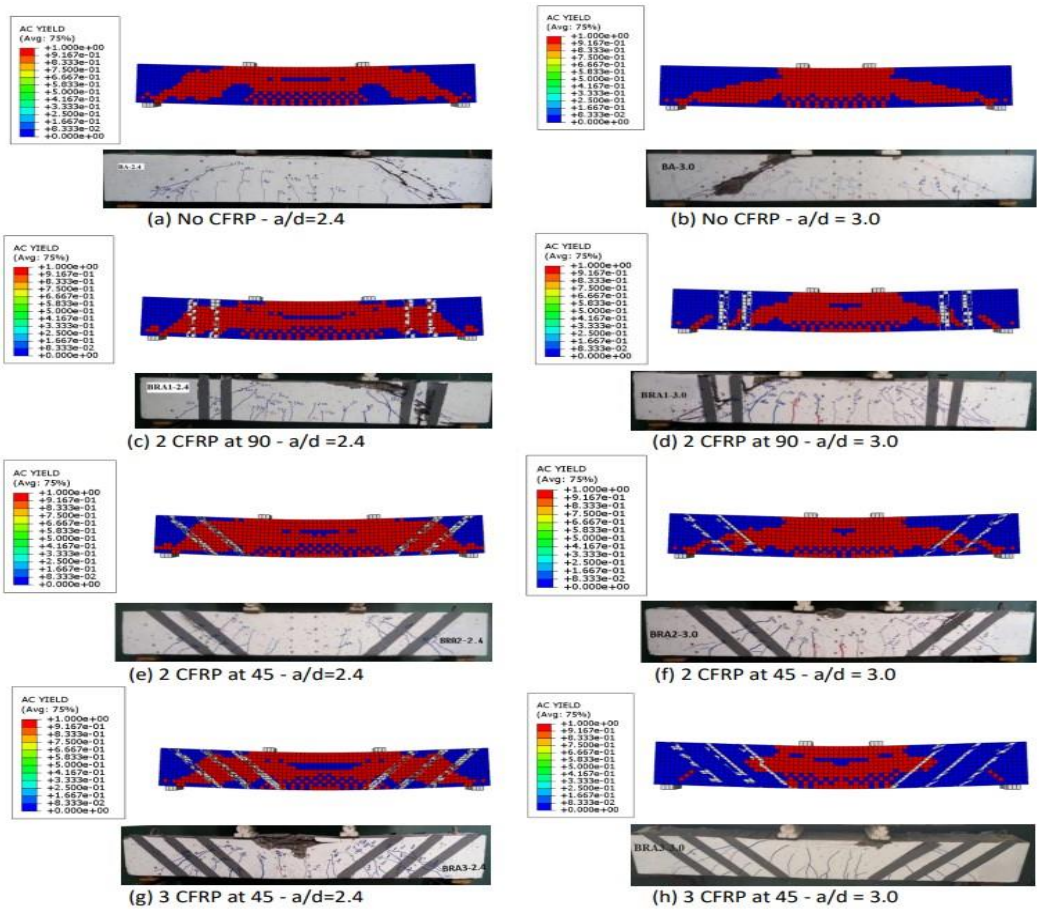

Figure 11. A cracking pattern of the beams in experiments and in FEA

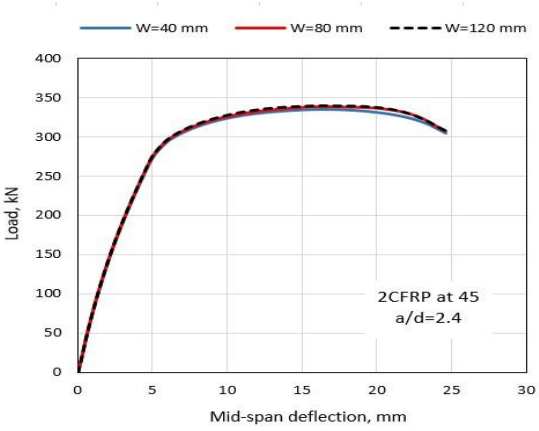

Figure 12. Load–deflection relationship in case of changing CFRP width

Therefore, the second parameter adopted is changing concrete compressive strength. Three compressive strengths are examined, and the results are shown in Table 7.

Upon decreasing concrete compressive strength, the maximum loading that withstands by the beam decreases. The deflection also decreases with decreasing compressive strength. Reducing the concrete compressive strength by 10 MPa and 20 MPa from 72.5 MPa decreases the beam loading tolerance by about (4-6) % and (10-12) % at both cracking and ultimate states, respectively. However, the failure pattern does not change.

The effect of compressive strength and the accompanying change in the tensile strength is on resisting the stresses transmitted through the beam section along its length and reaching the maximum stress the beam can bear. Therefore, lowering the compressive strength causes a lowering of the maximum stress that the beam can withstand.

Figures 13-16 show the load-deflection relationships for the control and rehabilitated beams with CFRP sheets at a/d of 2.4 and 3.0. Adding CFRP sheets to retrofit the beams can slightly enhance the ductility of the beams, but to a specific limit due to the linear behavior of CFRP until failure.

TABLE 7. Effect of variation of concrete compressive strength on retrofitted beams

Beam ID	f'c = 52.5 MPa				f'c = 62.5 MPa				f'c = 72.5 MPa			
	Pcr, kN	Δcr, mm	Pu, kN	Δu, mm	Pcr, kN	Δcr, mm	Pu, kN	Δu, mm	Pcr, kN	Δcr, mm	Pu, kN	Δu, mm
BA-2.4	50.9	0.74	242.3	10.30	55.4	0.74	256.5	12.65	57.7	0.74	272.8	13.25
BRA1-2.4	52.5	0.74	286.7	13.10	55.6	0.74	303.5	14.48	58.4	0.74	319.6	15.78
BRA2-2.4	52.8	0.74	302.6	13.24	55.8	0.74	321.8	15.27	58.5	0.74	334.9	16.41
BRA3-2.4	53.1	0.74	330.6	14.86	56.1	0.74	351.5	16.45	58.8	0.74	370.7	17.81

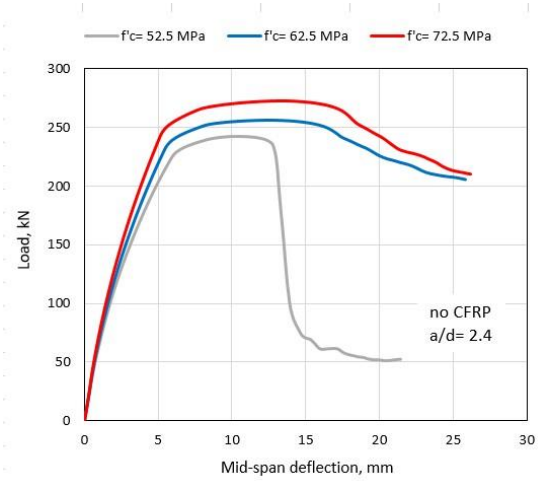

Figure 13. Load-deflection relationship of beams without CFRP

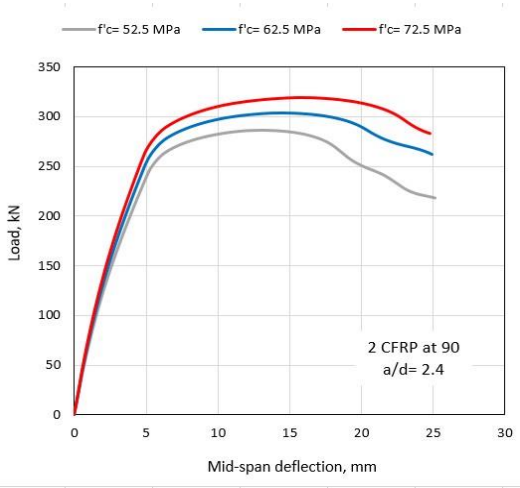

Figure 14. Load-deflection relationship of beams with vertical CFRP

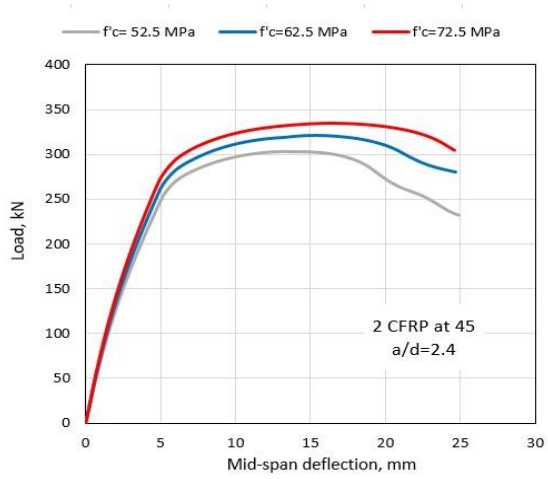

Figure 15. Load-deflection relationship of beams with two inclined CFRP at 45

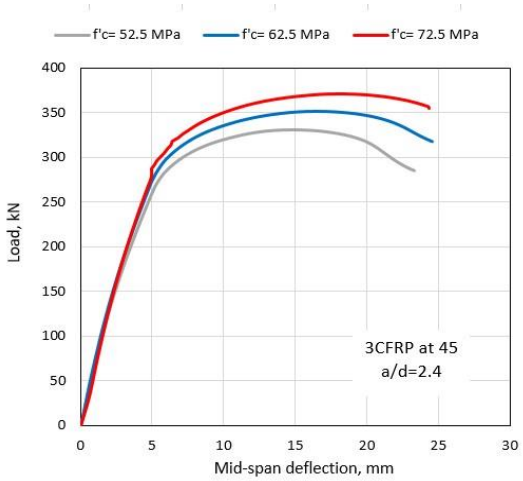

Figure 16. Load-deflection relationship of beams with three inclined CFRP at 45

6. CONCLUSIONS

This paper introduces a numerical investigation of using CFRP sheets to retrofit high-strength concrete beams after exposure to preload of 60 % of the ultimate resisting load. Three configurations of CFRP sheets and two a/d ratios are adopted to show their effects on the beam behavior. The FE results were compared and matched with the results of a previously implemented work. Two further parameters are tested. These are the CFRP sheet's width and concrete compressive strength. The following conclusions can reach:

Using CFRP sheets to retrofit cracked beams raises the ultimate load that the beam can bear. The increment

in peak load depends on the number and configuration of the attached CFRP sheets. Upon using 2 vertical sheets, 2-inclined at 45, and 3- inclined at 45 sheets, they can raise the ultimate load by (13-17) %, (19-23) %, and (35-36) %, respectively, for a/d of 2.4 and 3.0.

For a/d of 2.4, the impact of CFRP on shear resistance is more pronounced than for a/d of 3.0. When a/d increases, the loading capacity of the beam decreases by a range od (18-23) %. Also, the inclined sheets are more effective than the perpendicular ones.

The deflection corresponding to maximum loading increases according to CFRP sheets numbers and orientation. The increment ranges between (16-25) % for a/d of 2.4 and between (18-37) % for a/d of 3.0.

The failure of retrofitted beams was due to the yielding of longitudinal rebars, while the shear rebars did not yield.

Altering CFRP sheet width did not affect the beam tolerance for the applied load. However, increasing concrete compressive strength increases the beam tolerance for loading. Increasing the compressive strength by 10 MPa and 20 MPa raises beam capacity for loading by (4-6) % and (10-12) % at cracking and ultimate states, respectively.

7. REFERENCES

1. Gemert, D., "Design applications and durability of plate bonding technique", in Proceedings of the International Conference on Concrete Repair, Rehabilitation and Protection, Scotland. London: Chapman & Hall. (1996), 559-569.
2. Abbas, S., Ali, I. and Abdulridha, A., "Behavior and strength of steel fiber reinforced self-compacting concrete columns wrapped by carbon fiber reinforced polymers strips", ***International Journal of Engineering, Transactions B: Applications,***, Vol. 34, No. 2, (2021), 382-392. doi: 10.5829/IJE.2021.34.02B.10.
3. Täljsten, B., "Strengthening of existing concrete structures by epoxy bonded steel plates of steel or fibre reinforced plastics", in International Conference Radical Concrete Technology: 24/06/1996-28/06/1996, Taylor and Francis Group. (1996), 623-632.
4. Faez, A., Sayari, A. and Manei, S., "Retrofitting of rc beams using reinforced self-compacting concrete jackets containing aluminum oxide nanoparticles", ***International Journal of Engineering, Transactions B: Applications,***, Vol. 34, No. 5, (2021), 1195-1212. doi: 10.5829/ije.2021.34.05b.13.
5. Osman, B.H., Wu, E., Ji, B. and Abdulhameed, S.S., "Repair of pre-cracked reinforced concrete (RC) beams with openings strengthened using frp sheets under sustained load", ***International Journal of Concrete Structures and Materials***, Vol. 11, (2017), 171-183. doi: 10.1007/s40069-016-0182-3.
6. Rahimi, S.B., Jalali, A., Mirhoseini, S.M. and Zeighami, E., "Experimental comparison of different types of frp wrapping in repairing of rc deep beams with circular openings", ***International Journal of Engineering, Transactions B: Applications,***, Vol. 34, No. 8, (2021), 1961-1973. doi: 10.5829/ije.2021.34.08b.17.
7. Miller, M. and Frye, M., "Scc proves successful in repair and strengthening projects", ***Concrete Construction Website***, (2009).
8. Daniel, I.M., Ishai, O., Daniel, I.M. and Daniel, I., "Engineering mechanics of composite materials, Oxford university press New York, Vol. 1994, (2006).
9. Soudki, K. and Alkhrdaji, T., "Guide for the design and construction of externally bonded frp systems for strengthening concrete structures (aci 440.2 r-02)", in Structures Congress 2005: Metropolis and Beyond. (2005), 1-8.
10. Haj Seiyed Taghia, S.A., Darvishvand, H.R. and Pourhasan, M., "An economic approach to the confinement of different concrete classes with carbon and glass fibers reinforced polymers", ***International Journal of Engineering, Transactions A: Basics***, Vol. 36, No. 4, (2023), 776-787. doi: 10.5829/ije.2023.36.04a.14.
11. Osman, B.H., Wu, E., Ji, B. and S Abdelgader, A.M., "A state of the art review on reinforced concrete beams with openings retrofitted with frp", ***International Journal of Advanced Structural Engineering***, Vol. 8, (2016), 253-267. doi: 10.1007/s40091-016-0128-7.
12. Ali, A., Abdalla, J., Hawileh, R. and Galal, K., "Cfrp mechanical anchorage for externally strengthened rc beams under flexure", ***Physics Procedia***, Vol. 55, (2014), 10-16. doi: 10.1016/j.phpro.2014.07.002.
13. Hafiz, T., "Life prediction of carbon fiber reinforced polymers using time temperature shift factor", ***International Journal of Engineering, Transactions A: Basics***, Vol. 33, No. 7, (2020), 1340-1346. doi: 10.5829/ije.2020.33.07a.21.
14. Mhanna, H.H., Hawileh, R.A. and Abdalla, J.A., "Shear strengthening of reinforced concrete beams using cfrp wraps", ***Procedia Structural Integrity***, Vol. 17, (2019), 214-221. doi: 10.1016/j.prostr.2019.08.029.
15. Mohsenzadeh, S., Maleki, A. and Lotfollahi-Yaghin, M., "Strengthening of rc beams using scc jacket consisting of glass fiber and fiber-silica fume composite gel", ***International Journal of Engineering, Transactions B: Applications,*** Vol. 34, No. 8, (2021), 1923-1939. doi: 10.5829/ije.2021.34.08b.14.
16. Kaw, A.K., "Mechanics of composite materials, CRC press, (2005).
17. AlSaeedi, A., "Shear retrofitting of reinforced high strength concrete beams using cfrp", MSc Thesis, Civil Engineering Department, University of Technology, Iraq: 172, (2017),
18. Committee, A., "Building code requirements for structural concrete (aci 318-08) and commentary, American Concrete Institute. (2008).
19. Standard, A., *C31/c31m, 2010," standard practice for making and curing concrete test specimens in the field," astm international, west conshohocken, pa, 2010, doi: 10.1520/c0031_c0031m*.
20. Pawar, A.J., Patel, M. and Suryawanshi, S., "Finite element modelling of laboratory tests on reinforced concrete beams containing recycled aggregate concrete", ***International Journal of Engineering, Transactions B: Applications,***, Vol. 36, No. 5, (2023), 991-999. doi: 10.5829/ije.2023.36.05b.15.
21. Inc, A., "Abaqus version 6.10-1 analysis user's manual", ***Dassault Systèmes Simulia Corp***, Vol. 3, (2017), 1-10. doi.
22. Abulqasim, S.A., Noori, A.Q.N. and Çelik, T., "Numerical investigation on flexural behavior of rc beams wıth large web opening externally strengthened wıth cfrp lamınates under cyclıc load: Three-poınt bendıng test", (2022). doi: 10.5937/jaes0-32985.
23. Paul, S.K. and Sahu, P., "Finite element analysis of retrofitting of rc beam with cfrp using abaqus", ***International Research Journal of Engineering and Technology (IRJET),*** Vol. 7, No., (2020), 1268-1273.
24. Aljazaeri, Z. and Al-Jaberi, Z., "Numerical study on flexural behavior of concrete beams strengthened with fiber reinforced cementitious matrix considering different concrete compressive strength and steel reinforcement ratio", ***International Journal of Engineering***, Vol. 34, No. 4, (2021), 793-802. doi: 10.5829/ije.2021.34.04a.05.
25. Zhang, D., Wang, Q. and Dong, J., "Simulation study on cfrp strengthened reinforced concrete beam under four-point

bending", ***Computers and Concrete***, Vol. 17, No. 3, (2016), 407-421. doi: 10.12989/cac.2016.17.3.407.

26. Ibrahim, S.K. and Rad, M.M., "Numerical plastic analysis of non-prismatic reinforced concrete beams strengthened by carbon fiber reinforced polymers", in Proceedings of the 13th fib International PhD Symposium in Civil Engineering, Marne-la-Vallée, Paris, France. (2020), 26-28.
27. Beckett, D. and Alexandrou, A., "Introduction to eurocode 2: Design of concrete structures (including seismic actions), New York, (1997).
28. Mahdi, A.M., "Impact of failure-surface parameters of concrete damage plasticity model on the behavior of reinforced ultra-high performance concrete beams", ***Periodica Polytechnica Civil Engineering***, Vol. 67, No. 2, (2023), 495-504. doi: 10.3311/PPci.21345.
29. Jabbar, A.M., Danha, L.S. and Hasan, Q.A., "Numerical simulation of ultra-high-performance concrete's compressive and tensile behaviour in beams", ***Journal of Applied Engineering Science***, Vol. 21, No. 2, (2023), 532-546. doi: 10.5937/jaes0-40769.
30. Systèmes, D., "Getting started with abaqus: Interactive edition 6.12", ***Getting Started with Abaqus: Interactive Edition***, Vol., (2012), 4.50-54.54. http://www.maths.cam.ac.uk/computing/software/abaqus_docs/docs/v6.12/pdf_books/GET_STARTED.pdf
31. Kumar, N.M., Sameer, S. and Divya, K., "Numerical simulations of composite materials", in IOP Conference Series: Earth and Environmental Science, IOP Publishing. Vol. 982, (2022), 012019.

Persian Abstract

چکیده

هدف این مقاله بررسی عددی رفتار ساختاری تیرهای بتن با مقاومت بالا (HSC) مقاوم‌سازی‌شده توسط ورق‌های پلیمر تقویت‌شده با فیبر کربن (CFRP) پس از ترک‌خوردگی است. شش تیر HSC پیش‌ترک‌شده مجهز به ورق‌های CFRP که دارای تقویت‌کننده‌های یکسان هستند، به‌علاوه دو تیر دیگر بدون CFRP به‌عنوان تیرهای کنترل، به‌صورت عددی با بارگذاری چهار نقطه‌ای تا زمان شکست با استفاده از نرم‌افزار Abaqus آزمایش می‌شوند. ورق های CFRP در سه طرف تیر در دهانه برشی پس از ترک در زیر ۶۰ درصد بارگذاری متصل می شوند. دو فاصله دهانه برشی، دو شیب صفحات CFRP، و تعداد ورق‌ها به عنوان پارامترهایی برای مقایسه با نتایج تجربی به‌دست‌آمده قبلی اتخاذ می‌شوند. نتایج آزمایش با یافته های عملی برای کالیبره کردن پارامترهای Abaqus مطابقت دارد. نتایج نشان می‌دهد که مقاوم‌سازی تیر ترک خورده توسط CFRP تحمل آن را در برابر بار اعمال شده با دامنه (۳۶-۱۳) درصد بسته به نسبت دهانه برشی به عمق و آرایش ورق‌های CFRP افزایش می‌دهد. هنگامی که تیر در برش تمایل به شکست دارد، اثر CFRP نسبت به زمانی که تمایل به شکستگی در خمش دارد، بارزتر است. ورق های شیبدار نسبت به ورق های عمودی موثرتر هستند. علاوه بر این، دو پارامتر اضافی برای روشن شدن اثرات آنها بر رفتار تیرهای مقاوم سازی شده در نظر گرفته شده است: عرض ورق و مقاومت فشاری بتن. تغییر عرض CFRP بر تحمل تاثیر نمی گذارد، در حالی که افزایش مقاومت فشاری بتن بارگذاری تیر را افزایش می دهد.